Dengue Virus Nonstructural Protein 5 Adopts Multiple Conformations in Solution

ARTICLE *in* BIOCHEMISTRY · JULY 2012

Impact Factor: 3.02 · DOI: 10.1021/bi300406n · Source: PubMed

2 AUTHORS, INCLUDING:

Kyung H Choi
University of Texas Medical Branch at Galveston
30 PUBLICATIONS **857** CITATIONS

BIOCHEMISTRY
including biophysical chemistry & molecular biology

Article

pubs.acs.org/biochemistry

Dengue Virus Nonstructural Protein 5 Adopts Multiple Conformations in Solution

Cécile Bussetta and Kyung H. Choi*

Department of Biochemistry and Molecular Biology, Sealy Center for Structural Biology and Molecular Biophysics, University of Texas Medical Branch, Galveston, Texas 77555-0647, United States

ABSTRACT: Dengue virus (DENV) nonstructural protein 5 (NS5) is composed of two globular domains separated by a 10-residue linker. The N-terminal domain participates in the synthesis of a mRNA cap 1 structure (^{7Me}GpppA$_{2'OMe}$) at the 5′ end of the viral genome and possesses guanylyltransferase, guanine-N7-methyltransferase, and nucleoside-2′O-methyltransferase activities. The C-terminal domain is an RNA-dependent RNA polymerase responsible for viral RNA synthesis. Although crystal structures of the two isolated domains have been obtained, there are no structural data for full-length NS5. It is also unclear whether the two NS5 domains interact with each other to form a stable structure in which the relative orientation of the two domains is fixed. To investigate the structure and dynamics of DENV type 3 NS5 in solution, we conducted small-angle X-ray scattering experiments with the full-length protein. NS5 was found to be monomeric and well-folded under the conditions tested. The results of these experiments also suggest that NS5 adopts multiple conformations in solution, ranging from compact to more extended forms in which the two domains do not seem to interact with each other. We interpret the multiple conformations of NS5 observed in solution as resulting from weak interactions between the two NS5 domains and flexibility of the linker in the absence of other components of the replication complex.

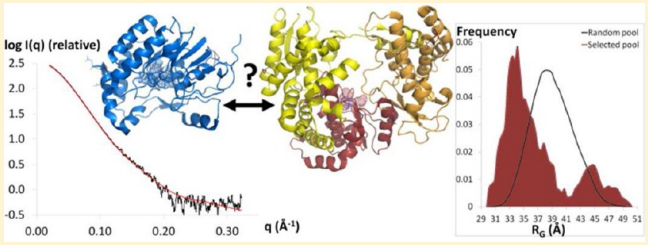

Dengue infection is the most prevalent arthropod-borne disease in the world, with 50−100 million cases of infection annually and approximately 2.5 billon people at risk of infection.[1,2] Because of the dramatic increase in its incidence around the world over the past 25 years, dengue is classified by the Centers for Disease Control and Prevention (CDC) as an emerging infectious disease.[3,4] Dengue infection results in a wide spectrum of clinical manifestations that range from asymptomatic to life-threatening disease, often associated with unpredictable clinical evolution and outcome.[2] The World Health Organization (WHO) currently classifies symptomatic infections in three categories: undifferentiated fever, a flu-like dengue fever, and dengue hemorrhagic fever (DHF) characterized by plasma leakage. The most serious complication of DHF is dengue shock syndrome (DSS), which occurs when signs of circulatory failure are detected in addition to other DHF symptoms.[2,5] Dengue is caused by four serologically different types of dengue virus, DENV-1−DENV-4, and while infection with one of the four DENV serotypes provides lifelong immunity to that serotype, a secondary infection with another serotype results in a greater risk for developing DHF and DSS. Despite the significant health impact of dengue infections, neither an effective vaccine, which must confer immunity to all four serotypes, nor a specific antiviral therapy is available.[2,3]

Dengue viruses belong to the flavivirus genus in the Flaviviridae family, which includes other major human pathogens such as yellow fever, West Nile, Japanese encephalitis, and tick-borne encephalitis viruses.[1,4] The flavivirus genome is a positive sense single-stranded RNA that acts as a mRNA upon infection.[6] Similar to most cellular mRNAs, the flavivirus genome is capped on the 5′ end with a cap 1 structure that consists of a 7-methylguanosine linked to the genome via a 5′−5′ triphosphate link with a methyl group added onto 2′O of the genomic 5′-terminal nucleotide, which is an adenine in all flaviviruses.[7] The genome thus consists of the 5′-cap 1 structure (^{7Me}GpppA$_{2'OMe}$), a 5′-untranslated region (5′-UTR), a single open reading frame (ORF), and a 3′-untranslated region (3′-UTR), but unlike cellular mRNAs, flavivirus genomes do not contain a poly-A tail on their 3′ ends.[6] After translation of the ORF by the host machinery, the resulting polyprotein is processed by cellular and viral proteases into three structural proteins (C, prM, and E) and seven nonstructural proteins (NS1, NS2A, NS2B, NS3, NS4A, NS4B, and NS5).[6] Nonstructural proteins NS1, NS2A, NS3, NS4A, and NS5, along with the viral RNA and host proteins, associate into a viral replicase in a modified membrane structure derived from the endoplasmic reticulum.[6,8] Among the nonstructural proteins, the two-domain proteins NS3 and NS5 are the key enzymes in the replication complex, as together they account for all activities needed for genome replication and cap synthesis.[9,10] NS3 (~70 kDa) consists of an N-terminal serine protease domain, which requires NS2B as a cofactor, and a C-terminal domain possessing three distinct activities: an RNA

Received: March 30, 2012
Revised: July 2, 2012
Published: July 3, 2012

   dx.doi.org/10.1021/bi300406n | *Biochemistry* 2012, 51, 5921−5931

helicase, RNA-stimulated nucleoside triphosphatase (NTPase), and 5′-RNA triphosphatase (5′-RTPase).[10] NS5, the largest NS protein (~103 kDa), consists of an N-terminal domain possessing three activities necessary for cap synthesis (guanylyltransferase, guanine-N7-methyltransferase, and nucleoside-2′O-methyltransferase) and a C-terminal domain that harbors the primer-independent RNA-dependent RNA polymerase (RdRp) activity.[10−13] This latter domain is responsible for the replication of the positive-strand RNA genome in an asymmetric and semiconservative process in which the antigenome is present in only a double-stranded RNA replication intermediate.[6] During replication, the helicase activity of the NS3 C-terminal domain is thought to be involved in unwinding the replicative form. After replication of the viral genome by the NS5 RdRp domain, the cap structure is added onto the 5′ end of the genome by four enzyme activities.[14] First, the 5′ γ-phosphate of the RNA genome is cleaved by the NS3 C-terminal domain to produce a diphosphate-terminated RNA (ppAX$_n$, where X$_n$ represents the RNA). Second, the NS5 guanylyltransferase/methyltransferase (GTase/MTase) domain catalyzes the transfer of a GMP moiety from GTP to the RNA. The third and fourth activities are two *S*-adenosyl-L-methionine (SAM)-dependent methylations, also catalyzed by the NS5 GTase/MTase domain. These methylations occur sequentially, with guanine N7 methylation preceding the nucleoside 2′O methylation.[14] Genome capping likely occurs during the initial stages of replication, but little is known about how flaviviruses coordinate these two processes.

The interdependence of the NS3 and NS5 activities, suggested by the sequence of reactions during genome replication and capping, was shown by experiments in which NS5 stimulates NS3's NTPase and 5′-RTPase activities,[15−17] and NS3 stimulates NS5's GTase activity.[12] Moreover, multiple experiments (e.g., co-immunoprecipitation and pull-down assays in DENV-infected cells) demonstrate that NS3 and NS5 interact with each other.[16−18] The modularity of NS3 is functionally relevant because the protease domain influences the activities and specificity of the helicase/NTPase/5′-RTPase domain.[16,19−22] In contrast, the linkage between the two NS5 domains does not seem to be relevant to the function of these two domains, because the RdRp activity is not altered by the presence of the GTase/MTase domain, and the GTase and MTase activities are not affected by the RdRp domain.[12,23] While three structures of full-length NS3 have been determined in two different conformations,[20,22,24] only the structures of the two isolated NS5 domains have been determined,[25,26] and there is no structural information available for full-length NS5. The NS5 N-terminal GTase/MTase domain has a globular shape with dimensions of 55 Å × 45 Å × 40 Å and has a fold similar to the SAM-dependent methyltransferase fold[25,27] (Figure 1). Biochemical and structural analyses identified K61-D146-K182-E218 (KDKE motif) as the active site residues of the nucleoside-2′O-MTase activity, while only D146 is essential for the guanine-N7-MTase activity.[28] The guanylyltransferase catalytic residue has been proposed to be K29,[12,13] though this residue is not conserved among the flavivirus NS5 sequences and the reaction mechanism remains uncertain. The NS5 C-terminal RdRp domain has the characteristic shape of the DNA/RNA polymerase superfamily (structural classification of proteins database),[29] commonly compared to a right hand with fingers, palm, and thumb subdomains and overall dimensions of 65 Å × 60 Å × 40 Å[26] (Figure 1). However, RdRps differ from other polymerases of the same superfamily in that they adopt a

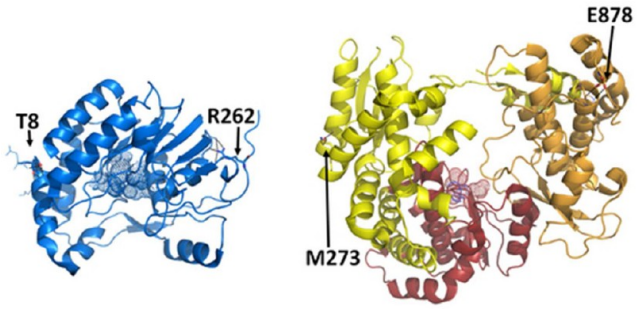

Figure 1. Crystal structures of NS5 GTase/MTase (left) and RdRp (right) domains. The RdRp subdomains are colored yellow, red, and orange for the fingers, palm, and thumb subdomains, respectively. Active site residues are represented as spheres, and residues at the extremities of each domain are represented as sticks and labeled accordingly.

"closed-hand" conformation, which results from an extension of the fingers subdomain, called the fingertips, connecting the thumb subdomain.[26,30,31] The active site of the RdRp domain is contained in the palm subdomain where the conserved RdRp motif C (GDD motif, G662-D663-D664) is found. In all primer-independent RdRp structures, the active site is encircled by the fingers and thumb subdomains, the fingertips, and a thumb protrusion that occlude the proposed dsRNA product exit site.[30,31] Thus, structural and biochemical analyses of Flaviviridae RdRps suggest that large conformational changes are required during the exit of the dsRNA product.[30−33]

Herein, we report the first structural analysis of full-length DENV-3 NS5 in solution using small-angle X-ray scattering (SAXS). Our results indicate that NS5 is monomeric in solution, as described previously.[34] The low-resolution shape of NS5 in solution, which resembles an asymmetric and elongated spheroid, has a volume that can accommodate the crystal structures of the DENV NS5 GTase/MTase and RdRp domains very well. However, the relative orientation of the two domains could not be determined accurately. Because the refinement of an atomic model directly against the experimental data is more reliable than docking domain structures into a low-resolution SAXS-derived shape, we used this strategy to compare our SAXS data to a previously published model of a flavivirus NS5[35] and to generate alternate models by rigid-body modeling. In addition, we analyze the flexibility of NS5 in solution and demonstrate that it can adopt conformations ranging from compact to more extended forms, with a predominance of compact forms. Overall, our results suggest that in absence of any other protein or nucleic acids, the two domains of NS5 do not interact tightly with each other and that the nonconserved linker is flexible in solution.

EXPERIMENTAL PROCEDURES

Expression and Purification of NS5$_{1-878}$. The DNA fragment encoding DENV-3 NS5$_{1-878}$ (residues 1−878) was amplified via polymerase chain reaction from the full-length clone (900 residues) and subcloned into a pET28a vector (EMD biosciences) containing the coding sequence for six histidines and a thrombin cleavage site at the 5′ end of the cloning site. Recombinant NS5$_{1-878}$ was produced in BL21-CodonPlus-RIL *Escherichia coli* cells (Stratagene). The culture was grown in Luria Broth (LB) medium supplemented with 25 μg/mL chloramphenicol and 50 μg/mL kanamacyn at 37 °C until an absorbance (at 600 nm) of 0.6 was reached. Protein

expression was induced by addition of 1 mM isopropyl 1-thio-β-D-galactopyranoside at 18 °C overnight. Cell pellets were collected by centrifugation (5000 rpm for 30 min) and resuspended in lysis buffer [50 mM sodium phosphate (pH 7) and 1.3 M NaCl] complemented with 1 mg/mL lysozyme, 10 μg/mL ribonuclease A, and one tablet of protease inhibitor cocktail (Roche Applied Science). After incubation for 20 min at 4 °C, the cell lysate was sonicated and clarified by centrifugation (17600*g* for 30 min). $NS5_{1-878}$ was first purified by cobalt metal affinity chromatography (TALON metal affinity resin, Clontech) using an imidazole gradient from 5 to 150 mM in 0.75 M NaCl and 25 mM sodium phosphate buffer (pH 7). This was followed by size-exclusion chromatography (SEC) purification using HiLoad 16/60 Superdex 200 preparative grade (GE Healthcare) equilibrated in SEC buffer [25 mM Tris-HCl (pH 7), 400 mM NaCl, 5% glycerol, and 2 mM DTT]. The homogeneity of the protein was then assessed by densitometry on denaturing polyacrylamide gel electrophoresis (SDS−PAGE) and by detection of a single species by analytical ultracentrifugation (AUC) (data not shown), in accordance with previously published results for $NS5_{1-900}$.[34] The protein concentration was determined by UV absorbance at 280 nm with a NanoDrop 1000 spectrophotometer (Thermo Scientific) and a theoretical molar extinction coefficient of 210708 M^{-1} cm^{-1}.

Collection and Evaluation of SAXS Data. SAXS experiments were performed on ALS beamline 12.3.1 (SIBYLS, Lawrence Berkeley National Laboratory, Berkeley, CA). Scattering intensities $I(q)$ for protein and buffer samples were recorded as a function of scattering vector q ($q = 4\pi \sin\theta/\lambda$, where 2θ is the scattering angle and λ is the X-ray wavelength). The sample-to-detector distance was set to 1.5 m, which resulted in a q range of 0.01−0.32 $Å^{-1}$; λ was 1.0 Å, and all experiments were performed at 20 °C. The data collection strategy described by Hura et al.[36] was used in this study. Briefly, SAXS data were collected for three protein concentrations (1.2, 1.8, and 3.5 mg/mL) to evaluate the effects of concentration on the scattering curves and for two buffer samples (SEC buffer) to minimize errors due to instrumentation. For each sample measurement, SAXS data were collected for three X-ray exposures: one long exposure (5 s) flanked by two short exposures (0.5 s) to assess radiation damage. Scattering contributions of the SEC buffer were subtracted from sample scattering data using ogreNew (SIBYLS beamline). Data analysis was performed using PRIMUS from ATSAS suite 2.3.[37] Experimental SAXS data obtained for the different protein concentrations were analyzed for aggregation and folding state using Guinier and Kratky plots, respectively. The forward scattering intensity $I(0)$ (also called the extrapolated scattering intensity at zero angle) and the radius of gyration R_G were evaluated using the Guinier approximation: $I(q) \approx I(0) \exp[(-q^2R_G^2)/3]$, with the limit $qR_G < 1.3$. These parameters were also determined from the pair-distance distribution function $P(R)$, which was calculated from the entire scattering pattern via indirect Fourier inversion of the scattering intensity $I(q)$ using GNOM.[38] The maximal particle diameter D_{max} was also estimated from $P(R)$. The hydrated volume V_p of the particle was computed from the Porod invariant and was used to estimate the molecular mass of a globular protein. Indeed, it was empirically found that the hydrated volume in cubic nanometers should numerically be between 1.5 and 2 times the molecular mass in kilodaltons.[39] The apparent molecular mass was also determined from $I(0)$ using the formula $MM_p = MM_{st}\{[I(0)_p/c_p]/[I(0)_{st}/c_{st}]\}$, where MM, $I(0)$, and c are the molecular mass, the forward scattering intensity, and the concentration of the protein of interest (subscript p) or the standard protein (subscript st), respectively.[40] Lysozyme (2, 3, and 6 mg/mL) and bovine serum albumin (1 and 2 mg/mL) were used as standard proteins.

SAXS Data Analysis. The overall shape of the protein was modeled ab initio by fitting the SAXS data to the calculated SAXS profile of a chainlike ensemble of dummy residues in reciprocal space using GASBOR, version 2.2i.[41] The radius of the volume in which dummy atoms are placed is determined by $D_{max}/2$. Ten independent calculations were performed with no symmetry restrictions. The agreement between the three-dimensional model and the SAXS data was determined using the discrepancy χ^2, defined according to Konarev et al.,[37] and the molecular envelope showing the lower χ^2 was chosen as the reference model. Suite DAMAVER was then used to align the molecular envelopes, select the most typical ones, and build an averaged model.[42] The alignment of two molecular envelopes was conducted by minimizing the value of the normalized spatial discrepancy (NSD), which indicates that two shapes are similar when the NSD value is close to 1.[42] The R_G and D_{max} values of the averaged model were calculated using CRYSOL.[43] The atomic structures of both domains [Protein Data Bank (PDB) entry 1L9K for the GTase/MTase domain and PDB entry 2J7U for the RdRp domain] were fit into the averaged molecular envelope using SUPCOMB.[44] SASREF[45] was used to calculate a model that best fits to the experimental SAXS data (minimization of discrepancy χ^2) while agreeing with a previously proposed model based on results from genetic interaction experiments.[35] The tertiary structure of $NS5_{1-878}$ was also modeled using the crystal structures of the individual domains and BUNCH.[45] This program performs modeling of multidomain proteins against SAXS data using a combined rigid body for the atomic structures of the domains and an ab initio modeling approach for regions of unknown structure. As with the GASBOR calculations, 10 independent models were generated, and the comparison between atomic structures of models and the envelope calculated by GASBOR was conducted using SUPCOMB as described above. To assess the flexibility of this two-domain protein, we employed the EOM (Ensemble Optimization Method) suite,[46] which can be used to select the best-fitting conformational ensemble when the atomic structures of globular domains are known. First, RanCh (Random Chain) creates 10000 randomized models with different conformations of the linker and protein extremities. GAJOE (Genetic Algorithm Judging Optimization of Ensembles) selects a pool of models that best fit the experimental curve. The dimensions of models from the selected pool are then compared to those from the random pool to evaluate protein flexibility. For rigid-body calculations, domain extremities were chosen on the basis of comparison of all available crystal structures for each flavivirus NS5 domain.[13,47−50] The GTase/MTase domain included residues between T8 and R262, and the RdRp domain comprised residues between M273 and E878 (last residue of the construct).

RESULTS

$NS5_{1-878}$ Is Monomeric in Solution, As Determined by SAXS Experiments. The quality of the SAXS measurements was estimated by comparing data from different exposure times and different concentrations. No radiation damage was detected

dx.doi.org/10.1021/bi300406n | Biochemistry 2012, 51, 5921−5931

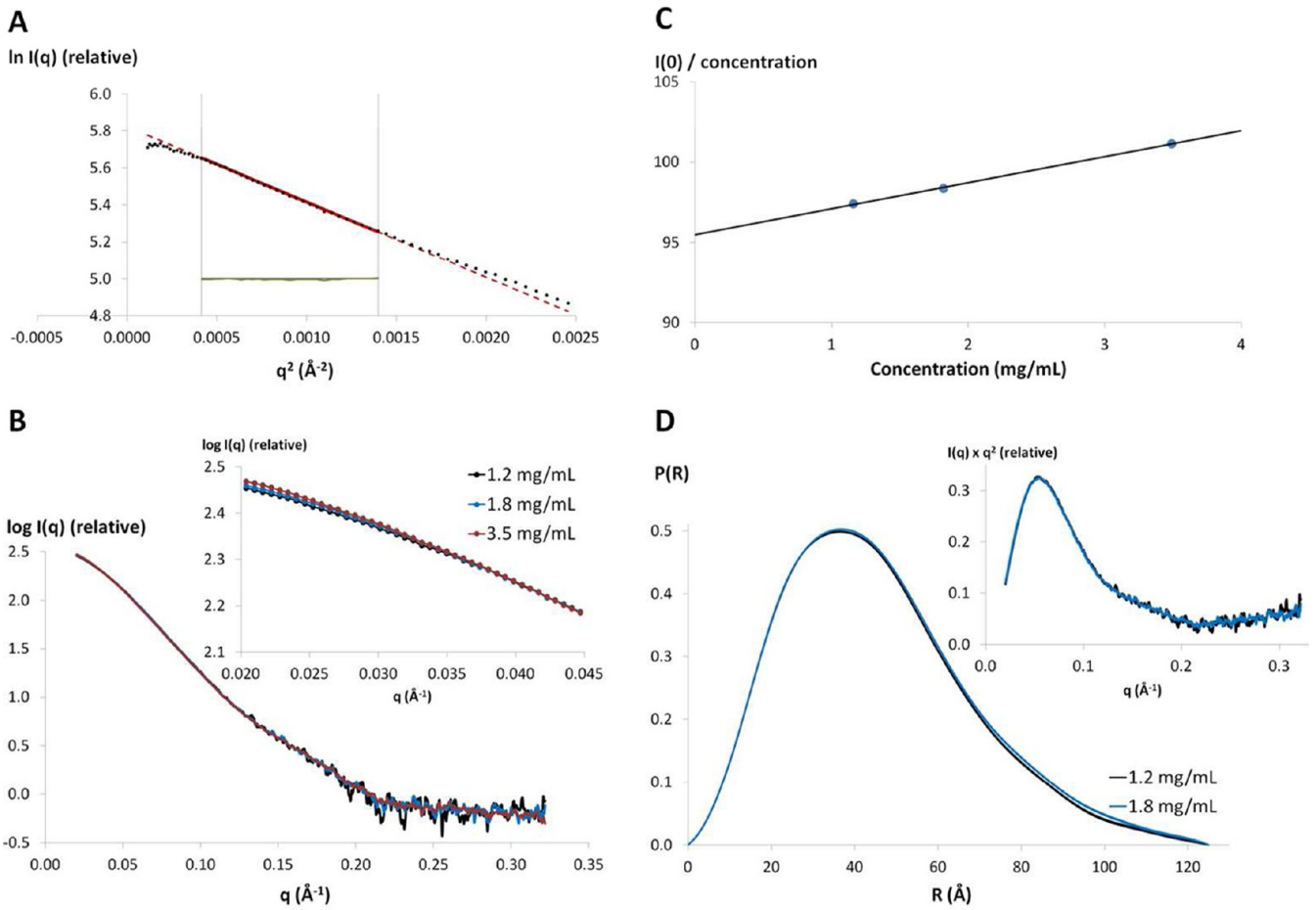

Figure 2. SAXS data analysis. (A) Guinier plot of the scattered intensities of $NS5_{1-878}$ at 1.2 mg/mL (·). The Guinier region ($qR_G < 1.3$) is delimited by the gray vertical lines. The red solid line is the linear regression fit in the Guinier region, expanded by a red dashed line. The residuals are colored green. (B) Experimental scattering patterns for three concentrations of $NS5_{1-878}$ scaled to concentration. The concentration dependence of the scattering curves at very low scattering angles is shown in the inset. (C) Concentration dependence of $I(0)$/concentration, where $I(0)$ is the forward scattering intensity derived using the Guinier law. (D) Pair-distance distribution function $P(R)$ of $NS5_{1-878}$ at 1.2 and 1.8 mg/mL. Kratky plots of $NS5_{1-878}$ SAXS data at 1.2 and 1.8 mg/mL are shown in the inset.

Table 1. Parameters Derived from SAXS Data for Three Concentrations of $NS5_{1-878}$ and Extrapolated to Zero Concentration[a]

	"0" mg/mL	1.2 mg/mL	1.8 mg/mL	3.5 mg/mL
R_G (Guinier[37]) (Å)	34.4 ± 1	35.1 ± 1	35.4 ± 1	36.4 ± 1
R_G [$P(R)$[38]] (Å)	35.0 ± 1	35.6 ± 1	36.1 ± 1	36.9 ± 1
D_{max} [$P(R)$[38]] (Å)	–	125	125	135
V_p (Porod[37]) (nm^3)	151.4	155.6	155.9	162.2
molecular mass [$I(0)$[37]] (kDa)	95.5 ± 10	97.4 ± 10	98.4 ± 10	101.1 ± 10
molecular mass (Porod[37]) (kDa)	88.3 ± 13	90.8 ± 13	90.9 ± 13	94.6 ± 13
oligomerization state	monomer	monomer	monomer	monomer

[a]The methods used to determine the parameters are given.

over the 5 s exposure time, so the data obtained after the long exposure were used for analysis. Several parameters describing the shape, size, and volume can be extracted directly from scattering curves, but only if the solution is monodisperse. NS5 eluted from SEC as a single peak corresponding to the size of a monomer. After concentration of the protein fractions, the sample homogeneity and purity were estimated by densitometry on SDS−PAGE (>97% pure). The monodispersity and the monomeric state of $NS5_{1-878}$ were then confirmed by analytical ultracentrifugation (data not shown). The linearity of the Guinier plot {ln[$I(q)$] vs q^2} for $qR_G < 1.3$ also indicated the quality of the sample[51] (Figure 2A). A minor concentration dependence was observed at a very small angle for scattering vectors ($q < 0.035$ Å) (Figure 2B,C), while at larger angles, the scattering curves superimposed well when the data were scaled for concentration (Figure 2B). This concentration dependence, indicating a slight attractive interparticle interference, appeared to be linear to a good approximation ($R^2 = 0.9988$) (Figure 2C) and so can be eliminated by extrapolating the experimental data to zero concentration.[52] The SAXS parameters extrapolated to zero concentration were within the margin of error of those calculated from 1.2 and 1.8 mg/mL samples (Table 1), suggesting that the scattering curves at these concentrations can be considered free from any interparticle interference.

dx.doi.org/10.1021/bi300406n | *Biochemistry* 2012, 51, 5921−5931

Two parameters addressing the size of the particle in solution, the radius of gyration (R_G) and the maximal dimension (D_{max}), were determined from the SAXS data. First, the value of R_G can be obtained using two independent methods: the Guinier approximation, where only the innermost portion of the scattering curve is used, and the pair-distribution function $P(R)$, which has the advantage of taking into account the whole scattering curve. Both methods provided values in good agreement with each other: 35.1 ± 1 and 35.6 ± 1 Å, respectively, at 1.2 mg/mL and 35.4 ± 1 and 36.1 ± 1 Å, respectively, at 1.8 mg/mL. These values are also in agreement with those obtained by extrapolating to zero concentration: 34.4 ± 1 and 35.0 ± 1 Å, respectively (Table 1). Next, the maximal dimension of the particle, D_{max}, was estimated from the pair-distance distribution function $P(R)$, which represents the probable distribution of interatomic distances. D_{max} was found to be 125 ± 10 Å for both 1.2 and 1.8 mg/mL protein solutions (Figure 2D). The molecular mass of an object in solution can also be determined from two independent measurements: the forward scattering intensity $I(0)$ and the hydrated particle volume (V_P). Apparent molecular masses estimated from $I(0)$ were 97.4 ± 10 and 98.4 ± 10 kDa for 1.2 and 1.8 mg/mL samples, respectively. The hydrated particle volumes estimated from Porod plots were 155.6 nm^3 at 1.2 mg/mL and 155.9 nm^3 at 1.8 mg/mL, corresponding to average molecular masses of 90.8 ± 13 and 90.9 ± 13 kDa, respectively (Table 1). These values, as well as the extrapolated molecular mass at zero concentration [95.5 ± 10 kDa (Table 1)], are consistent with the value of 103 kDa, calculated from the amino acid sequence. These results thus indicate that $NS5_{1-878}$ is monodisperse and monomeric in solution at both 1.2 and 1.8 mg/mL. The shape and other modeling calculations presented below were based on the experimental data collected with the 1.2 mg/mL sample, which are very similar to those based on the data set of the 1.8 mg/mL sample (data not shown).

Ab Initio Shape Calculations of $NS5_{1-878}$. The shape of $NS5_{1-878}$ in solution can be estimated from the shapes of the Kratky plot and the pair-distance distribution function $P(R)$. The Kratky plot [$I(q) \times q^2$ vs q] (Figure 2D, inset) shows a bell-shaped peak at low angles that indicates a well-folded protein, and the pair-distance distribution function $P(R)$ shows a characteristic shape of a prolate spheroid (Figure 3).[39,53] A better approximation of the $NS5_{1-878}$ shape was then obtained using GASBOR. Ten independent ab initio reconstructions of the $NS5_{1-878}$ envelope produced a similar ellipsoidal envelope [NSD = 1.2 ± 0.1 (see Experimental Procedures)], in accordance with the prediction from the shape of the pair-distance distribution function. These models fit the experimental data well, as shown by the fit between the calculated SAXS profile from the reference model and the measured SAXS data [χ^2 of 1.3 (Figure 3)]. The averaged model has a relatively flat and asymmetric shape, with a larger bulge at one extremity (Figure 3, inset). The R_G and D_{max} of the averaged shape are 34.6 and 125.6 Å, respectively, as calculated from the coordinate file (see Experimental Procedures). The crystal structures of the individual domains have disklike shapes, although the GTase/MTase domain (55 Å × 45 Å × 40 Å, PDB entry 1L9K) is significantly smaller than the RdRp domain (65 Å × 60 Å × 40 Å, PDB entry 2J7U). On the basis of these crystal structures, the averaged model was divided into two portions that seem to correspond to the GTase/MTase domain for the smaller part and to the RdRp domain for the larger part (Figure 3). The crystal structures fit the shape well,

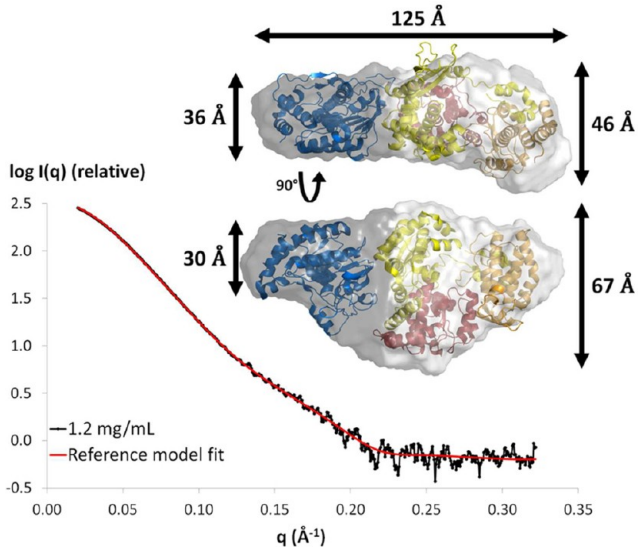

Figure 3. Ab initio shape determination of $NS5_{1-878}$. Fit of the SAXS profile derived from the ab initio reference model (red curve, χ^2 = 1.3) to the experimental scattering curve of $NS5_{1-878}$ at 1.2 mg/mL (black). The inset shows two views of the averaged molecular envelope rotated by 90° from each other shown as surface representations, with fitted crystal structures of GTase/MTase and RdRp domains (same color code as in Figure 1).

but the precise mutual arrangement of the domains could not be determined without ambiguity, even when using a distance restriction (between 10 and 35 Å[54]) that mimics the 10-residue linker. This is likely due to the overall globular shape of each domain and the low resolution of SAXS-derived shapes.

Comparison of the SAXS Data with a Previously Published Model. In 2007, Malet et al.[35] published a structural model of full-length NS5 from West Nile virus, another member of the flavivirus family. The model was constructed on the basis of reverse genetic experiments that identified potentially interacting residues in the dengue virus GTase/MTase and RdRp domains. Specifically, the authors used the proposed interaction between residues K46, R47, and E49 from the GTase/MTase domain and residue L512 from the RdRp domains to build their model by protein−protein docking. Two distance restraints were applied during modeling: (a) a restraint of 36 Å between the C-terminal end of the GTase/MTase domain and the N-terminal end of the RdRp domain and (b) a restraint of 6 Å between residues K46, R47, and E49 from the GTase/MTase domain and residue L512 from the RdRp domain. To determine whether the published model of the full-length NS5 structure is consistent with the SAXS data, we used rigid-body refinement implemented in SASREF. Indeed, rather than comparing the structure of the published model directly with the SAXS data, SASREF was used to perform rigid-body modeling to generate a model that satisfies the same distance restraints as the published model while fitting the SAXS data. The structure of the DENV-3 GTase/MTase domain was generated by homology modeling based on the DENV-2 GTase/MTase crystal structure (PDB entry 1L9K). This homology model and the DENV-3 RdRp crystal structure (PDB entry 2J7U) were used in the SASREF calculations. The model that complies with the distance restraints and best fits the data does so very poorly, with a χ^2 of 6 (Figure 4A). This indicates that the previously proposed

dx.doi.org/10.1021/bi300406n | Biochemistry 2012, 51, 5921−5931

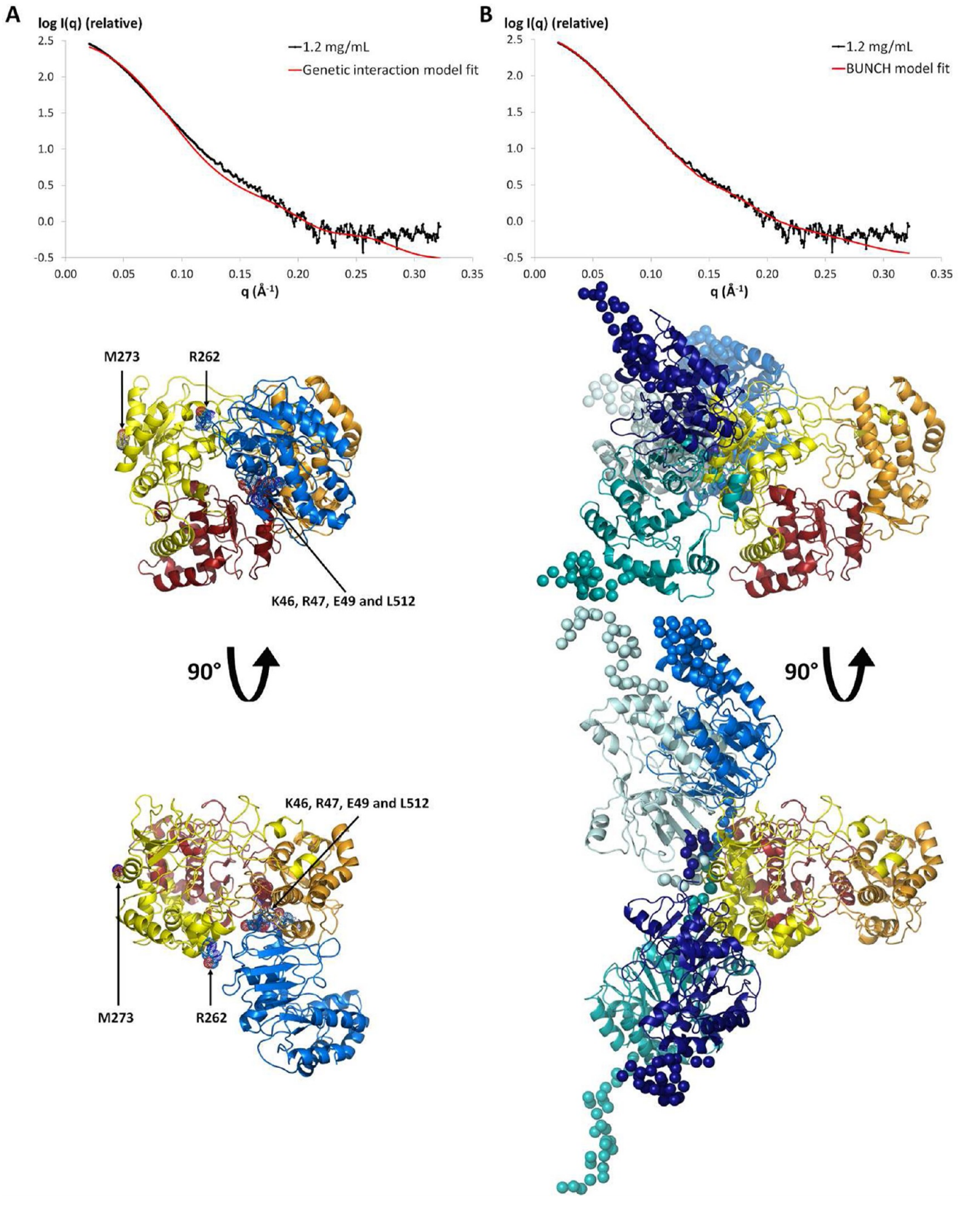

Figure 4. Comparison of the $NS5_{1-878}$ models with SAXS data. (A) Fit of the SAXS profile derived from the "genetic interaction" restrained rigid-body model (red curve, χ^2 = 6.0) to the experimental scattering curve of $NS5_{1-878}$ at 1.2 mg/mL (black). Two views of the atomic model are also shown (same color code as in Figure 1). (B) Fit of the scattering profile of the BUNCH model with the best χ^2 (red curve, χ^2 = 2.0) to the experimental scattering curve of $NS5_{1-878}$ at 1.2 mg/mL (black). Four models of 10 generated by BUNCH are superimposed. These four models were selected to highlight the variety of conformations obtained. The RdRp domains are colored as in Figure 1, and the GTase/MTase domains are colored in different shades of blue. The flexible regions are represented as spheres.

dx.doi.org/10.1021/bi300406n | *Biochemistry* 2012, 51, 5921−5931

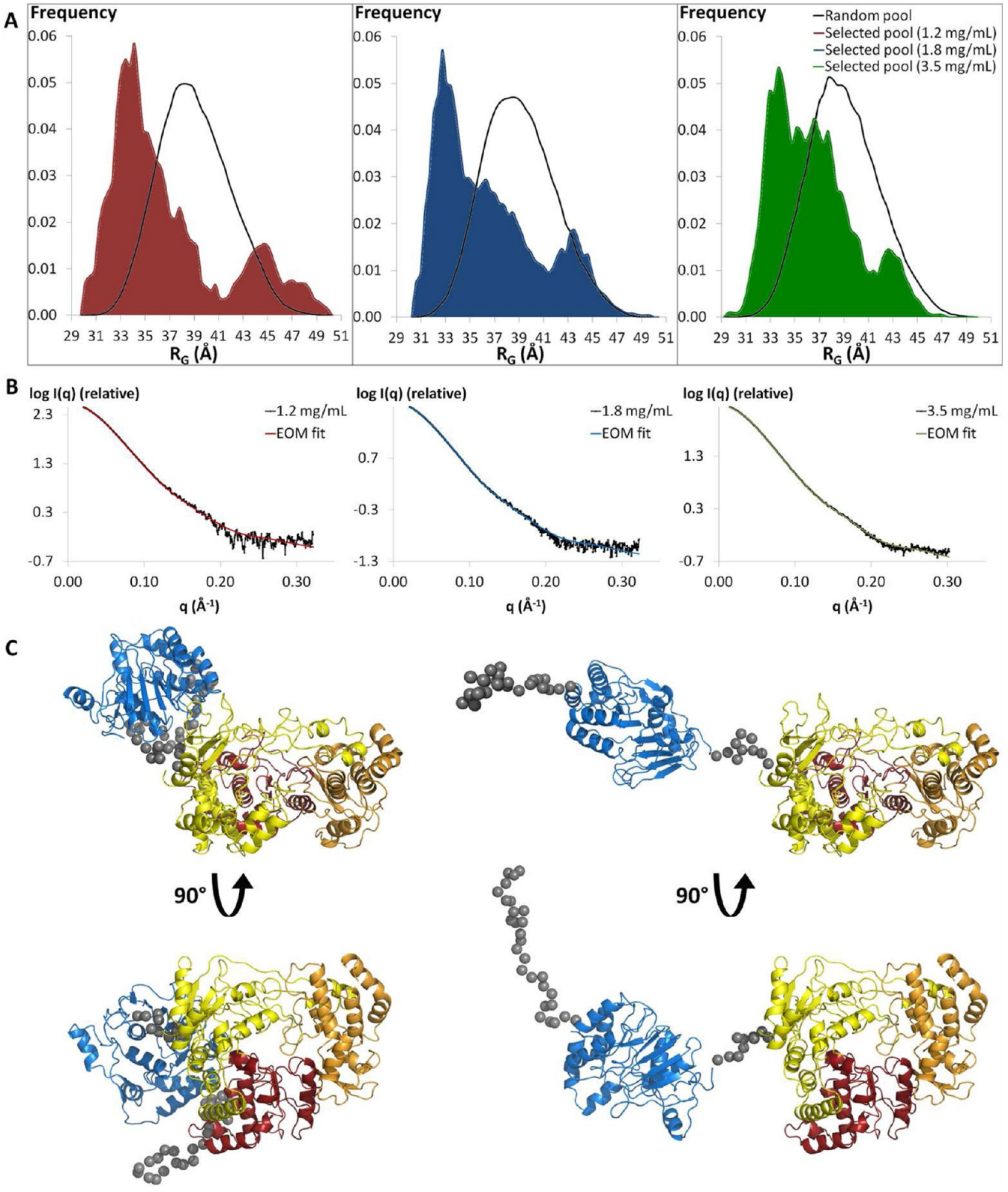

Figure 5. Multiple conformations of $NS5_{1-878}$. (A) Distributions of radii of gyration for the random (black) and selected (colored area) pools of $NS5_{1-878}$ structures for each concentration (red, blue, and green for 1.2, 1.8, and 3.5 mg/mL, respectively). (B) Fit of the scattering profile derived from the selected ensemble of conformations to the experimental scattering curve of $NS5_{1-878}$ at 1.2 mg/mL (red, χ^2 = 1.5), 1.8 mg/mL (blue, χ^2 = 1.2), and 3.5 mg/mL (green, χ^2 = 1.5). (C) Front and side views of two structures in the selected pool (1.2 mg/mL sample). A "compact conformation" (left, R_G = 33.9 Å, D_{max} = 120.3 Å) and an "extended conformation" (right, R_G = 44.6 Å, D_{max} = 163.3 Å) are shown with the same color code as in Figure 1. The flexible regions are represented as gray spheres.

dx.doi.org/10.1021/bi300406n | *Biochemistry* 2012, 51, 5921−5931

model alone could not explain the experimental SAXS data presented herein.

Rigid-Body Modeling of $NS5_{1-878}$. Ab initio calculations of the $NS5_{1-878}$ molecular envelope and comparison of SAXS data with a published NS5 model were not successful in producing an atomic model of $NS5_{1-878}$ in solution. Because it is more reliable to directly refine the relative positions of the two domains against the experimental data, a combination of rigid-body and ab initio modeling was performed, using BUNCH.[45] As described in Experimental Procedures, rigid-body modeling was applied to the domain structures (T8−R262 for the GTase/MTase domain and M273−E878 for the RdRp domain), and ab initio modeling was used for the N-terminal extremity (a total of 28 residues including a hexahistidine tag, a thrombin cleavage site, and residues G1−E7) as well as for the 10-residue linker (H263−N272). All 10 independent models showed a similar fit to the data, with χ^2 values ranging from 2.0 to 2.6 (Figure 4B). While the 10 calculations led to very different models in which the interdomain interaction surface varied significantly from one to the other, all the models present similarities to the averaged ab initio shape because they can be described as elongated, with the two domains arranged in a side-by-side configuration. In addition, the two NS5 domains interact with each other via a relatively small surface area (Figure 4B). In all these models, the fingers subdomain of the RdRp domain was always involved at the intermolecular interface, while the GTase/MTase domain displayed a variety of orientations.

Conformational Flexibility of $NS5_{1-878}$ in Solution. The modular organization of proteins is often associated with flexibility and multiple conformations in solution.[55] For $NS5_{1-878}$, the prolate ellipsoidal shape determined by GASBOR, the small and various interface between the two domains in the BUNCH models, and the absence of marked features (i.e., several peaks) in the Kratky plot and the $P(R)$ function may suggest a weak interaction between the two domains and thus the presence of flexibility in domain orientation.[39] We used EOM[46] to determine if these observations are due to linker flexibility that permits $NS5_{1-878}$ to adopt different conformations in solution. From an ensemble of random $NS5_{1-878}$ models in which the interdomain linker and the N-terminal extremity were allowed to have different conformations, EOM selected a subensemble of ∼20 models that best fit the experimental data [χ^2 = 1.5 (Figure 5)]. Comparing the R_G distribution of the selected ensemble against that of the random ensemble gives an indication of the flexibility of $NS5_{1-878}$ in solution. The random R_G distribution covers the R_G range from ∼30 to ∼50 Å, corresponding to compact to very extended conformations, respectively. In contrast, the R_G distribution of the selected pool has a bimodal distribution that could result from a linker region switching between two major conformations in solution. The first peak is relatively sharp and centered around an R_G of 33−34 Å and represents ∼80% of the selected ensemble of models. This suggests that the most highly populated conformations of $NS5_{1-878}$ are compact in solution. However, the R_G distribution contains a second small peak at 44−45 Å, which accounts for ∼20% of the subensemble of models (Figure 5).

To determine whether the presence of an extended conformation is an artifact from protein aggregation, EOM analysis was also performed on SAXS data obtained for higher protein concentrations [1.8 and 3.5 mg/mL (Figure 5)]. In both cases, the selected ensemble fit the SAXS data well with χ^2 values of 1.2 and 1.5 for the 1.8 and 3.5 mg/mL samples, respectively (Figure 5B). Similar to the EOM results from the 1.2 mg/mL sample, the R_G distribution is bimodal for both concentrations (Figure 5A). Additionally, the frequency of some "compact" conformations (34 Å < R_G < 41 Å) increased, while the proportion of "extended" conformations (R_G > 41 Å) decreased at higher concentrations. The extended conformations represent 18 and 12% of the selected pool of structures for concentrations of 1.8 and 3.5 mg/mL, respectively (Figure 5A). Taken together with the EOM results obtained for the concentration of 1.2 mg/mL, we found that the percentage of the population with extended conformations is linearly dependent on NS5 concentration to a good approximation (coefficient of determination R^2 of 0.996). Therefore, the percentage of the population in extended conformations was calculated to be 23.3% when extrapolated to zero concentration. Because the proportion of extended conformations does not increase as the protein concentration increases, we conclude that the observed extended population is not an artifact of interparticle interference or protein aggregation.

DISCUSSION

The dengue virus NS5 protein is the catalytic subunit of the viral replication complex and so is essential for viral transcription and genome replication. This critical protein is composed of two globular domains tethered by a 10-residue linker. Although their crystal structures have been determined separately,[25,26] little is known about the potential interaction between the two domains. To tackle this question in the absence of a crystal structure of full-length NS5, we performed SAXS experiments, because they are a powerful tool for obtaining structural information regarding the overall shape of objects in solution. Analysis of SAXS and analytical ultracentrifugation data clearly shows that $NS5_{1-878}$ is monomeric and monodisperse in solution under our experimental conditions. Multidomain proteins consisting of two or more folded domains joined by linkers represent a high fraction of proteins in the three kingdoms of life, with a prediction of 65% of the proteins in eukaryotes and 40% in bacteria and archaea.[55] This modular organization is often associated with flexibility and the presence of several protein conformations in solution.[46] Flexibility between the NS5 domains was established from SAXS data. Therefore, models obtained from ab initio shape calculations and rigid-body modeling represent an "average" of all $NS5_{1-878}$ conformations and do not reflect a unique structure of the protein in solution. Approximately 80% of $NS5_{1-878}$ ensemble structures have a relatively compact structure in which the two domains likely interact with each other. However, the broad R_G (from 30 to 41 Å) of this population hints at the existence of multiple conformations in solution, possibly with diverse contacts between the GTase/MTase and RdRp domains. More extended conformations of $NS5_{1-878}$, in which the two domains do not interact, represent ∼20% of $NS5_{1-878}$ ensemble structures in solution. These calculations suggest that the interaction between the GTase/MTase and RdRp domains may be transient and heterogeneous. Thus, even if the model proposed by Malet et al.[35] does not fit well with our SAXS data by itself, we cannot exclude the existence of such a conformation in solution and/or in the replication complex. The NS5 linker region (residues 263−273) was rarely observed in crystal structures of flavivirus NS5 domains. When it is seen in the structure, this region does not have any secondary structure and shows conformational

disorder, as observed in the crystal structures of the Wesselbron virus GTase/MTase domain.[13] In this latter structure, the linker is a loop connected to the first helix of the RdRp domain (residues 275−285), and these two regions show a higher degree of dynamics compared to the rest of the protein.[13] The high mobility of the C-terminal region of the Wesselbron virus GTase/MTase domain is in accordance with the SAXS data presented here indicating flexibility between the NS5 GTase/MTase and RdRp domains. Furthermore, activity assays indicate that the two domains are functionally independent of each other, because it was shown that the GTase/MTase domain does not affect RdRp activity[23] and that the RdRp domain does not affect GTase activity.[12] To fully understand the dynamics of NS5 and the importance of the linker for viral replication, it would be informative to test different sequences, lengths, or even the absence of the linker, in vitro and in the context of viral replication. Moreover, transcomplementation experiments between the two domains of NS5 would also be valuable for understanding why the GTase/MTase and RdRp domains are linked together. On the other hand, it has been shown that NS5 modulates NS3 NTPase and 5′-RTPase activities, and NS3 modulates NS5 GTase activity.[12,15−17] Interactions between NS5 and NS3 were also identified by different methods. For example, the NS3 C-terminal domain was shown to interact with residues from the NS5 fingers domain (residues 320−368) using the yeast two-hybrid system,[56] and a genetic interaction was demonstrated between the NS3 C-terminal domain and the NS5 GTase/MTase domain.[17,57] From these data, we propose that NS5 can adopt different conformations in solution, and the flexibility of the linker may be restrained upon interaction with NS3 or other components of the replication complex during the viral life cycle. A structure of the complex between NS5 and NS3 will provide key information regarding essential interaction sites that could become a target for the design of dengue replication inhibitors.

AUTHOR INFORMATION

Corresponding Author

*Address: 301 University Blvd., Galveston, TX 77555-0647. E-mail: kychoi@utmb.edu. Phone: (409) 747-1402. Fax: (409) 747-1406.

Funding

This work was supported by a University of Texas Medical Branch Sealy Memorial Endowment Fund research pilot grant and a National Institutes of Health Grant R01 AI-57363 (to K.H.C.) and supported in part by a Sealy and Smith Foundation grant to the Sealy Center for Structural Biology and Molecular Biophysics.

Notes

The authors declare no competing financial interest.

ACKNOWLEDGMENTS

We acknowledge SIBYLS beamline 12.3.1 at the Advanced Light Source (Lawrence Berkeley National Laboratory), where SAXS data were collected (Contract Number DE-AC02-05CH11231 with the U.S. Department of Energy). We especially thank Michal Hammel for assistance during data collection and Luis Holthauzen for help with AUC experiments and analysis. We are also very grateful to Mark White for helpful discussions and critical reading of the manuscript and David Konkel for critically editing it.

ABBREVIATIONS

AUC, analytical ultracentrifugation; DENV, dengue virus; DHF, dengue hemorrhagic fever; D_{max}, maximal dimension; DSS, dengue shock syndrome; GTase, guanylyltransferase; MTase, methyltransferase; NS, nonstructural protein; NSD, normalized spatial discrepancy; NTPase, RNA-stimulated nucleoside triphosphatase; ORF, open reading frame; $P(R)$, pair-distribution function; RdRp, RNA-dependent RNA polymerase; R_G, radius of gyration; 5′-RTPase, 5′-RNA triphosphatase; SEC, size-exclusion chromatography; SAM, *S*-adenosyl-L-methionine; SAXS, small-angle X-ray scattering; UTR, untranslated region; V_P, hydrated particle volume.

REFERENCES

(1) Gould, E. A., and Solomon, T. (2008) Pathogenic flaviviruses. *Lancet 371*, 500−509.

(2) World Health Organization (2009) Dengue: Guidelines for diagnosis, treatment, prevention and control; World Health Organization, Geneva.

(3) Mackenzie, J. S., Gubler, D. J., and Petersen, L. R. (2004) Emerging flaviviruses: The spread and resurgence of Japanese encephalitis, West Nile and dengue viruses. *Nat. Med. 10*, S98−S109.

(4) Vasilakis, N., and Weaver, S. C. (2008) The history and evolution of human dengue emergence. *Adv. Virus Res. 72*, 1−76.

(5) Rigau-Perez, J. G., Clark, G. G., Gubler, D. J., Reiter, P., Sanders, E. J., and Vorndam, A. V. (1998) Dengue and dengue haemorrhagic fever. *Lancet 352*, 971−977.

(6) Paranjape, S. M., and Harris, E. (2010) Control of dengue virus translation and replication. *Curr. Top. Microbiol. Immunol. 338*, 15−34.

(7) Khromykh, A. A., Kondratieva, N., Sgro, J. Y., Palmenberg, A., and Westaway, E. G. (2003) Significance in replication of the terminal nucleotides of the flavivirus genome. *J. Virol. 77*, 10623−10629.

(8) Fernandez-Garcia, M. D., Mazzon, M., Jacobs, M., and Amara, A. (2009) Pathogenesis of flavivirus infections: Using and abusing the host cell. *Cell Host Microbe 5*, 318−328.

(9) Perera, R., and Kuhn, R. J. (2008) Structural proteomics of dengue virus. *Curr. Opin. Microbiol. 11*, 369−377.

(10) Bollati, M., Alvarez, K., Assenberg, R., Baronti, C., Canard, B., Cook, S., Coutard, B., Decroly, E., de Lamballerie, X., Gould, E. A., Grard, G., Grimes, J. M., Hilgenfeld, R., Jansson, A. M., Malet, H., Mancini, E. J., Mastrangelo, E., Mattevi, A., Milani, M., Moureau, G., Neyts, J., Owens, R. J., Ren, J., Selisko, B., Speroni, S., Steuber, H., Stuart, D. I., Unge, T., and Bolognesi, M. (2009) Structure and functionality in flavivirus NS-proteins: Perspectives for drug design. *Antiviral Res. 87*, 125−148.

(11) Egloff, M. P., Decroly, E., Malet, H., Selisko, B., Benarroch, D., Ferron, F., and Canard, B. (2007) Structural and functional analysis of methylation and 5′-RNA sequence requirements of short capped RNAs by the methyltransferase domain of dengue virus NS5. *J. Mol. Biol. 372*, 723−736.

(12) Issur, M., Geiss, B. J., Bougie, I., Picard-Jean, F., Despins, S., Mayette, J., Hobdey, S. E., and Bisaillon, M. (2009) The flavivirus NS5 protein is a true RNA guanylyltransferase that catalyzes a two-step reaction to form the RNA cap structure. *RNA 15*, 2340−2350.

(13) Bollati, M., Milani, M., Mastrangelo, E., Ricagno, S., Tedeschi, G., Nonnis, S., Decroly, E., Selisko, B., de Lamballerie, X., Coutard, B., Canard, B., and Bolognesi, M. (2009) Recognition of RNA cap in the Wesselsbron virus NS5 methyltransferase domain: Implications for RNA-capping mechanisms in Flavivirus. *J. Mol. Biol. 385*, 140−152.

(14) Liu, L., Dong, H., Chen, H., Zhang, J., Ling, H., Li, Z., Shi, P. Y., and Li, H. (2010) Flavivirus RNA cap methyltransferase: Structure, function, and inhibition. *Front. Biol. 5*, 286−303.

(15) Cui, T., Sugrue, R. J., Xu, Q., Lee, A. K., Chan, Y. C., and Fu, J. (1998) Recombinant dengue virus type 1 NS3 protein exhibits specific viral RNA binding and NTPase activity regulated by the NS5 protein. *Virology 246*, 409−417.

(16) Yon, C., Teramoto, T., Mueller, N., Phelan, J., Ganesh, V. K., Murthy, K. H., and Padmanabhan, R. (2005) Modulation of the nucleoside triphosphatase/RNA helicase and 5′-RNA triphosphatase activities of Dengue virus type 2 nonstructural protein 3 (NS3) by interaction with NS5, the RNA-dependent RNA polymerase. *J. Biol. Chem. 280*, 27412−27419.
(17) Davidson, A. D. (2009) New Insights into Flavivirus Nonstructural Protein 5. In *Advances in Virus Research*, Chapter 2, pp 41−101, Academic Press, New York.
(18) Kapoor, M., Zhang, L., Ramachandra, M., Kusukawa, J., Ebner, K. E., and Padmanabhan, R. (1995) Association between NS3 and NS5 proteins of dengue virus type 2 in the putative RNA replicase is linked to differential phosphorylation of NS5. *J. Biol. Chem. 270*, 19100−19106.
(19) Xu, T., Sampath, A., Chao, A., Wen, D., Nanao, M., Chene, P., Vasudevan, S. G., and Lescar, J. (2005) Structure of the dengue virus helicase/nucleoside triphosphatase catalytic domain at a resolution of 2.4 Å. *J. Virol. 79*, 10278−10288.
(20) Luo, D., Xu, T., Hunke, C., Gruber, G., Vasudevan, S. G., and Lescar, J. (2008) Crystal structure of the NS3 protease-helicase from dengue virus. *J. Virol. 82*, 173−183.
(21) Chernov, A. V., Shiryaev, S. A., Aleshin, A. E., Ratnikov, B. I., Smith, J. W., Liddington, R. C., and Strongin, A. Y. (2008) The two-component NS2B-NS3 proteinase represses DNA unwinding activity of the West Nile virus NS3 helicase. *J. Biol. Chem. 283*, 17270−17278.
(22) Luo, D., Wei, N., Doan, D. N., Paradkar, P. N., Chong, Y., Davidson, A. D., Kotaka, M., Lescar, J., and Vasudevan, S. G. (2010) Flexibility between the protease and helicase domains of the dengue virus NS3 protein conferred by the linker region and its functional implications. *J. Biol. Chem. 285*, 18817−18827.
(23) Selisko, B., Dutartre, H., Guillemot, J. C., Debarnot, C., Benarroch, D., Khromykh, A., Despres, P., Egloff, M. P., and Canard, B. (2006) Comparative mechanistic studies of de novo RNA synthesis by flavivirus RNA-dependent RNA polymerases. *Virology 351*, 145−158.
(24) Assenberg, R., Mastrangelo, E., Walter, T. S., Verma, A., Milani, M., Owens, R. J., Stuart, D. I., Grimes, J. M., and Mancini, E. J. (2009) Crystal structure of a novel conformational state of the flavivirus NS3 protein: Implications for polyprotein processing and viral replication. *J. Virol. 83*, 12895−12906.
(25) Egloff, M. P., Benarroch, D., Selisko, B., Romette, J. L., and Canard, B. (2002) An RNA cap (nucleoside-2′-O-)-methyltransferase in the flavivirus RNA polymerase NS5: Crystal structure and functional characterization. *EMBO J. 21*, 2757−2768.
(26) Yap, T. L., Xu, T., Chen, Y. L., Malet, H., Egloff, M. P., Canard, B., Vasudevan, S. G., and Lescar, J. (2007) Crystal structure of the dengue virus RNA-dependent RNA polymerase catalytic domain at 1.85-angstrom resolution. *J. Virol. 81*, 4753−4765.
(27) Cheng, X., and Roberts, R. J. (2001) AdoMet-dependent methylation, DNA methyltransferases and base flipping. *Nucleic Acids Res. 29*, 3784−3795.
(28) Ray, D., Shah, A., Tilgner, M., Guo, Y., Zhao, Y., Dong, H., Deas, T. S., Zhou, Y., Li, H., and Shi, P. Y. (2006) West Nile virus 5′-cap structure is formed by sequential guanine N-7 and ribose 2′-O methylations by nonstructural protein 5. *J. Virol. 80*, 8362−8370.
(29) Lo Conte, L., Ailey, B., Hubbard, T. J., Brenner, S. E., Murzin, A. G., and Chothia, C. (2000) SCOP: A structural classification of proteins database. *Nucleic Acids Res. 28*, 257−259.
(30) Ferrer-Orta, C., Arias, A., Escarmis, C., and Verdaguer, N. (2006) A comparison of viral RNA-dependent RNA polymerases. *Curr. Opin. Struct. Biol. 16*, 27−34.
(31) Choi, K. H., and Rossmann, M. G. (2009) RNA-dependent RNA polymerases from Flaviviridae. *Curr. Opin. Struct. Biol. 19*, 746−751.
(32) Ferron, F., Bussetta, C., Dutartre, H., and Canard, B. (2005) The modeled structure of the RNA dependent RNA polymerase of GBV-C virus suggests a role for motif E in Flaviviridae RNA polymerases. *BMC Bioinf. 6*, 255.
(33) Cameron, C. E., Moustafa, I. M., and Arnold, J. J. (2009) Dynamics: The missing link between structure and function of the viral RNA-dependent RNA polymerase? *Curr. Opin. Struct. Biol. 19*, 768−774.
(34) Szymanski, M. R., Jezewska, M. J., Bujalowski, P. J., Bussetta, C., Ye, M., Choi, K. H., and Bujalowski, W. (2011) Full-length dengue virus RNA-dependent RNA polymerase-RNA/DNA complexes: Stoichiometries, intrinsic affinities, cooperativities, base, and conformational specificities. *J. Biol. Chem. 286*, 33095−33108.
(35) Malet, H., Egloff, M. P., Selisko, B., Butcher, R. E., Wright, P. J., Roberts, M., Gruez, A., Sulzenbacher, G., Vonrhein, C., Bricogne, G., Mackenzie, J. M., Khromykh, A. A., Davidson, A. D., and Canard, B. (2007) Crystal structure of the RNA polymerase domain of the West Nile virus non-structural protein 5. *J. Biol. Chem. 282*, 10678−10689.
(36) Hura, G. L., Menon, A. L., Hammel, M., Rambo, R. P., Poole, F. L., II, Tsutakawa, S. E., Jenney, F. E., Jr., Classen, S., Frankel, K. A., Hopkins, R. C., Yang, S. J., Scott, J. W., Dillard, B. D., Adams, M. W., and Tainer, J. A. (2009) Robust, high-throughput solution structural analyses by small angle X-ray scattering (SAXS). *Nat. Methods 6*, 606−612.
(37) Konarev, P. V., Volkov, V. V., Sokolova, A. V., Koch, M. H., and Svergun, D. I. (2003) PRIMUS: A Windows PC-based system for small-angle scattering data analysis. *J. Appl. Crystallogr. 36*, 1277−1282.
(38) Svergun, D. I. (1992) Determination of the regularization parameter in indirect-transform methods using perceptual criteria. *J. Appl. Crystallogr. 25*, 495−503.
(39) Mertens, H. D., and Svergun, D. I. (2010) Structural characterization of proteins and complexes using small-angle X-ray solution scattering. *J. Struct. Biol. 172*, 128−141.
(40) Mylonas, E., and Svergun, D. I. (2007) Accuracy of molecular mass determination of proteins in solution by small-angle X-ray scattering. *J. Appl. Crystallogr. 40*, s245−s249.
(41) Svergun, D. I., Petoukhov, M. V., and Koch, M. H. (2001) Determination of domain structure of proteins from X-ray solution scattering. *Biophys. J. 80*, 2946−2953.
(42) Volkov, V. V., and Svergun, D. I. (2003) Uniqueness of ab initio shape determination in small-angle scattering. *J. Appl. Crystallogr. 36*, 860−864.
(43) Svergun, D., Barberato, C., and Koch, M. H. J. (1995) CRYSOL: A Program to Evaluate X-ray Solution Scattering of Biological Macromolecules from Atomic Coordinates. *J. Appl. Crystallogr. 28*, 768−773.
(44) Kozin, M. B., and Svergun, D. I. (2001) Automated matching of high- and low-resolution structural models. *J. Appl. Crystallogr. 34*, 33−41.
(45) Petoukhov, M. V., and Svergun, D. I. (2005) Global Rigid Body Modeling of Macromolecular Complexes against Small-Angle Scattering Data. *Biophys. J. 89*, 1237−1250.
(46) Bernadó, P., Mylonas, E., Petoukhov, M. V., Blackledge, M., and Svergun, D. I. (2007) Structural Characterization of Flexible Proteins Using Small-Angle X-ray Scattering. *J. Am. Chem. Soc. 129*, 5656−5664.
(47) Assenberg, R., Ren, J., Verma, A., Walter, T. S., Alderton, D., Hurrelbrink, R. J., Fuller, S. D., Bressanelli, S., Owens, R. J., Stuart, D. I., and Grimes, J. M. (2007) Crystal structure of the Murray Valley encephalitis virus NS5 methyltransferase domain in complex with cap analogues. *J. Gen. Virol. 88*, 2228−2236.
(48) Geiss, B. J., Stahla, H., Hannah, A. M., Gari, A. M., and Keenan, S. M. (2009) Focus on flaviviruses: Current and future drug targets. *Future Med. Chem. 1*, 327−344.
(49) Jansson, A. M., Jakobsson, E., Johansson, P., Lantez, V., Coutard, B., de Lamballerie, X., Unge, T., and Jones, T. A. (2009) Structure of the methyltransferase domain from the Modoc virus, a flavivirus with no known vector. *Acta Crystallogr. D65*, 796−803.
(50) Bollati, M., Milani, M., Mastrangelo, E., de Lamballerie, X., Canard, B., and Bolognesi, M. (2009) Crystal structure of a methyltransferase from a no-known-vector Flavivirus. *Biochem. Biophys. Res. Commun. 382*, 200−204.

(51) Vachette, P., Koch, M. H., and Svergun, D. I. (2003) Looking behind the beamstop: X-ray solution scattering studies of structure and conformational changes of biological macromolecules. *Methods Enzymol. 374*, 584−615.
(52) Pilz, I. (1982) Small Angle X-ray Scattering. In *Proteins* (Glatter, O., and Kratky, O., Eds.) Chapter 8, pp 239−293, Academic Press Inc., London.
(53) Putnam, C. D., Hammel, M., Hura, G. L., and Tainer, J. A. (2007) X-ray solution scattering (SAXS) combined with crystallography and computation: Defining accurate macromolecular structures, conformations and assemblies in solution. *Q. Rev. Biophys. 40*, 191−285.
(54) George, R. A., and Heringa, J. (2002) An analysis of protein domain linkers: Their classification and role in protein folding. *Protein Eng. 15*, 871−879.
(55) Bernadó, P. (2010) Effect of interdomain dynamics on the structure determination of modular proteins by small-angle scattering. *Eur. Biophys. J. 39*, 769−780.
(56) Johansson, M., Brooks, A. J., Jans, D. A., and Vasudevan, S. G. (2001) A small region of the dengue virus-encoded RNA-dependent RNA polymerase, NS5, confers interaction with both the nuclear transport receptor importin-β and the viral helicase, NS3. *J. Gen. Virol. 82*, 735−745.
(57) Kroschewski, H., Lim, S. P., Butcher, R. E., Yap, T. L., Lescar, J., Wright, P. J., Vasudevan, S. G., and Davidson, A. D. (2008) Mutagenesis of the dengue virus type 2 NS5 methyltransferase domain. *J. Biol. Chem. 283*, 19410−19421.